© 2015. Published by The Company of Biologists Ltd | Journal of Cell Science (2015) 128, 4538-4549 doi:10.1242/jcs.174573

RESEARCH ARTICLE

AP-2-complex-mediated endocytosis of *Drosophila* Crumbs regulates polarity by antagonizing Stardust

Ya-Huei Lin[1], Heather Currinn[2], Shirin Meher Pocha[1], Alice Rothnie[2], Thomas Wassmer[2] and Elisabeth Knust[1,*]

ABSTRACT

Maintenance of epithelial polarity depends on the correct localization and levels of polarity determinants. The evolutionarily conserved transmembrane protein Crumbs is crucial for the size and identity of the apical membrane, yet little is known about the molecular mechanisms controlling the amount of Crumbs at the surface. Here, we show that Crumbs levels on the apical membrane depend on a well-balanced state of endocytosis and stabilization. The adaptor protein 2 (AP-2) complex binds to a motif in the cytoplasmic tail of Crumbs that overlaps with the binding site of Stardust, a protein known to stabilize Crumbs on the surface. Preventing endocytosis by mutation of AP-2 causes expansion of the Crumbs-positive plasma membrane domain and polarity defects, which can be partially rescued by removing one copy of *crumbs*. Strikingly, knocking down both AP-2 and Stardust leads to the retention of Crumbs on the membrane. This study provides evidence for a molecular mechanism, based on stabilization and endocytosis, to adjust surface levels of Crumbs, which are essential for maintaining epithelial polarity.

KEY WORDS: Crumbs, AP-2 complex, Endocytosis, Epithelial polarity, Stardust, PDZ-binding

INTRODUCTION

Epithelial tissues line the cavities and surfaces of most animals to compartmentalize the body and separate the interior from the external environment. Epithelial cells are highly polarized, with the apical membrane facing the outside or a lumen and the basolateral membrane contacting neighboring cells and the basement membrane. Apical and basolateral membrane domains perform distinct functions, which are ensured by their specific protein and lipid composition. Adherens junctions and tight junctions mark the boundary between apical and basal, and guarantee the integrity of epithelial tissues (reviewed in Knust and Bossinger, 2002; Rodriguez-Boulan and Macara, 2014; St Johnston and Ahringer, 2010; Tepass et al., 2001). An epithelial polarity program (EPP), consisting of a network of evolutionarily conserved proteins, ensures establishment and maintenance of epithelial polarity during tissue morphogenesis and homeostasis (Rodriguez-Boulan and Macara, 2014). One important player in the EPP is Crumbs (Crb), originally identified in *Drosophila*. Loss of function of *Drosophila crb* causes loss of apico-basal polarity and tissue integrity in many embryonic epithelia (Grawe et al., 1996; Jürgens et al., 1984; Tepass, 1996; Tepass and Knust, 1990), and comparable phenotypes are observed in mouse embryos lacking either *Crb2* or *Crb3*, two of the three mammalian *Crb* genes (Whiteman et al., 2014; Xiao et al., 2011). These results highlight the functional conservation from flies to mammals.

Drosophila Crb is a type I transmembrane protein, whose extracellular domain is composed of an array of epidermal growth factor (EGF)-like repeats, intermingled with repeats with similarity to the globular domain of laminin A. The short, highly conserved intracellular domain of Crb contains two functional motifs, a PDZ-domain-binding motif (PBM) and a protein 4.1, ezrin, radixin and moesin (FERM)-domain-binding motif (FBM). The FBM participates in regulating Hippo-mediated growth of wing imaginal discs (Chen et al., 2010; Ling et al., 2010; Ribeiro et al., 2014; Robinson et al., 2010) and is required for dorsal closure during embryogenesis (Klose et al., 2013). The PBM recruits the scaffolding protein Stardust (Sdt), which stabilizes Crb on the apical surface (Klose et al., 2013). Hence, loss of *sdt* mimics the *crb* mutant phenotype (Bachmann et al., 2001; Hong et al., 2001). Sdt associates with PATJ and Lin-7 (also known as Veli) to form the core of the Crb complex (reviewed in Bulgakova and Knust, 2009), whereas other proteins can transiently be recruited into the Crb complex, such as atypical protein kinase C (aPKC) or Par-6, which are members of the Par module (Kempkens et al., 2006; Nam and Choi, 2003).

Loss- and gain-of-function studies have shown that proper Crb levels on the apical plasma membrane are important for polarity. Lack of Crb can result in loss of the apical surface and impairment of the stability of adherens junctions in embryonic epithelia (Grawe et al., 1996; Tepass, 1996; Tepass et al., 1990). In contrast, Crb overexpression can induce the expansion of the apical surface, which eventually results in the disruption of the monolayered epithelial organization and/or tissue overproliferation (de Vreede et al., 2014; Fletcher et al., 2012; Klebes and Knust, 2000; Laprise et al., 2006; Lu and Bilder, 2005; Moberg et al., 2005; Pellikka et al., 2002; Tanentzapf et al., 2000; Wodarz et al., 1995). Crb overexpression in developing photoreceptor cells can generate a second apical pole (Muschalik and Knust, 2011). Therefore, it is not surprising that multiple mechanisms are put in place to regulate Crb levels on the apical surface, including stabilization at and trafficking to and from the membrane. A positive-feedback loop through homophilic interactions between extracellular domains of Crb in cis has been suggested to keep Crb on the apical membrane of follicle cells and thus ensures polarity (Fletcher et al., 2012). In addition, homophilic interactions in trans between the extracellular domains of Crb molecules on neighboring cells have been proposed to contribute to Crb stabilization on the apical membrane, both in *Drosophila* (Letizia et al., 2013; Röper, 2012) and in zebrafish (Zou et al., 2012).

Besides stabilization at the membrane, various steps on the trafficking pathway participate in fine-tuning the amount of Crb on the cell surface. Expression of dominant-negative forms of

[1]Max Planck Institute of Molecular Cell Biology and Genetics, Pfotenhauerstrasse 108, Dresden 01307, Germany. [2]School of Life and Health Sciences, Aston University, Aston Triangle, Birmingham B4 7ET, UK.

*Author for correspondence (knust@mpi-cbg.de)

Received 15 May 2015; Accepted 26 October 2015

Journal of Cell Science (2015) 128, 4538-4549 doi:10.1242/jcs.174573

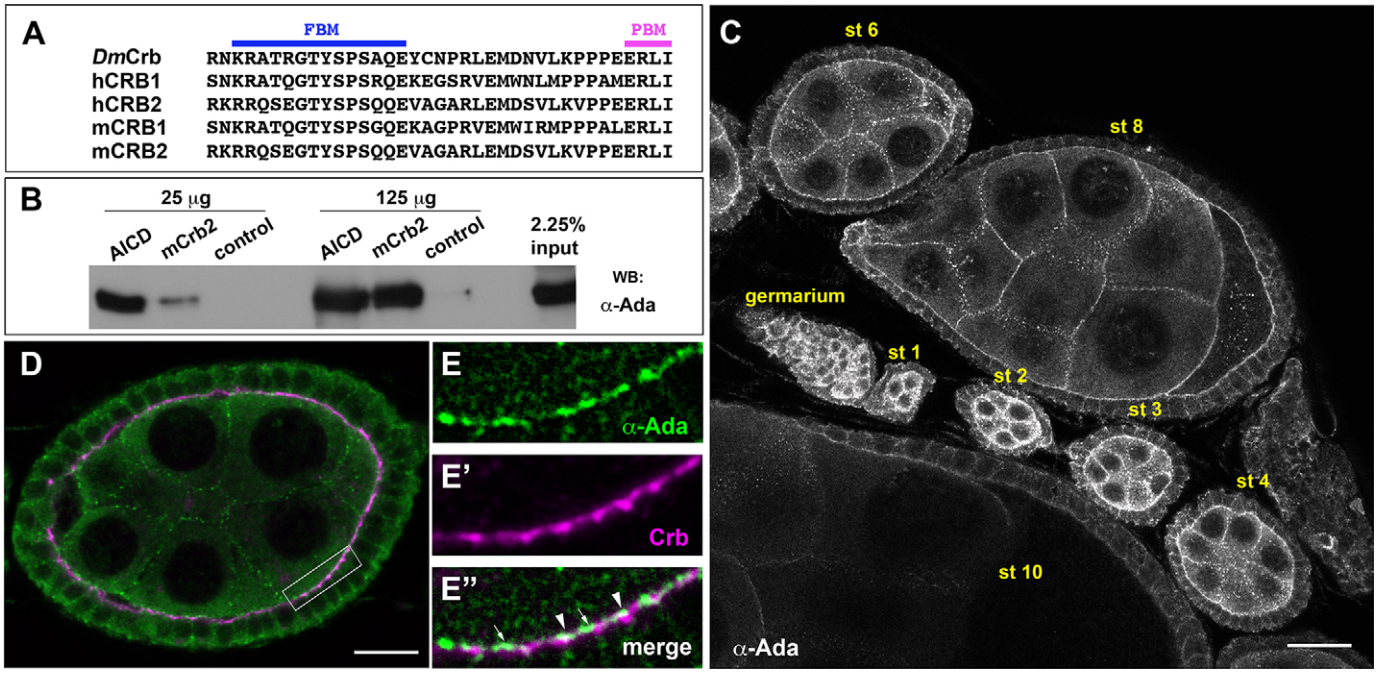

Fig. 1. α-Ada interacts with Crb. (A) Amino acid sequences of the cytoplasmic tails of *Drosophila melanogaster* Crb (*Dm*), and human (h) and mouse (m) Crb1 and Crb2. (B) Western blot of a proteo-liposome recruitment assay. mCrb2 tail coupled with liposomes was incubated with different amounts of adaptor mixture purified from pig brain. AICD is a positive control. (C) Wild-type follicle cells stained for α-Ada. Scale bar: 20 µm. (D,E) Wild-type follicle cells (stage 4) stained for α-Ada (D,E, green) and Crb (D,E′, magenta). Arrows, regions with no colocalization of Crb and α-Ada; arrowheads, regions where α-Ada and Crb colocalize. Scale bars: 10 µm.

Cdc42 or Rab11 results in depletion of Crb from the membrane and loss of apico-basal polarity in cells of the embryonic neuroectoderm (Harris and Tepass, 2008; Roeth et al., 2009). Similarly, blocking *Vps35*, a subunit of the retromer, which is involved in retrieval of transmembrane proteins from endosomes to the trans-Golgi network (TGN), causes loss of Crb from the apical membrane and disruption of epithelial polarity (Pocha et al., 2011; Zhou et al., 2011). Comparable phenotypes are observed in *Drosophila* epithelia that are mutant for αAdaptin (αAda, encoded by *AP-2α*), a constituent of the adaptor protein 2 (AP-2) complex (de Vreede et al., 2014) and in epithelia lacking Shrub (also known as Vps32), an ESCRT III component involved in endocytic sorting of membrane-bound proteins to lysosomal degradation. These data underscore the importance of regulating Crb levels on the apical surface to ensure polarity and tissue homeostasis.

To unravel in more detail the molecular mechanisms by which endocytosis regulates Crb levels, we analyzed the molecular and functional interaction between Crb and AP-2, a complex involved in clathrin-mediated endocytosis (Matsui and Kirchhausen, 1990; reviewed in Boehm and Bonifacino, 2001; Godlee and Kaksonen, 2013; Maldonado-Báez and Wendland, 2006; Reider and Wendland, 2011; Traub, 2009). The AP-2 complex comprises the large α and β2 subunits, the medium μ2 subunit and the small σ2 subunit. Using antibody uptake assays in garland cells, we show that *AP-2α* controls endocytosis of Crb. Liposome recruitment assays revealed a direct interaction between the cytoplasmic domain of Crb and the AP-2 complex through the PBM of Crb, hence the same motif that binds to Sdt. Strikingly, although loss of Sdt resulted in loss of Crb from the apical membrane, simultaneous reduction of both Sdt and αAda prevented surface depletion of Crb in wing-disc epithelia. These results show that the Crb–Sdt interaction prevents internalization of Crb by the AP-2 complex.

RESULTS

α-Ada associates with Crb

Given the observation that endocytic regulation of Crb is involved in regulating apical Crb levels, we asked whether Crb is a cargo for the AP-2 complex, an adaptor involved in internalization of transmembrane proteins. For this, we used the recently described proteo-liposome recruitment assay (Pocha et al., 2011). Given that the amino acid sequence of the intracellular tails of all Crb proteins are highly conserved from *Drosophila* to mammals (Fig. 1A), we incubated mouse Crb2 (mCrb2) tail-coupled liposomes with an adaptor mixture isolated from pig brain (Baust et al., 2006; Crottet et al., 2002). This mixture was highly enriched in constituents of the AP-2 complex (Fig. S1A,B). As positive control, we used the amyloid precursor protein intracellular domain (AICD), which contains a classical YxxF motif, and is internalized through clathrin-coated pits (Müller and Wild, 2013). This assay showed that mCrb2 tails interact with the AP-2 complex (Fig. 1B).

Next, we investigated the subcellular localization of α-Ada and Crb in *Drosophila* follicular cells, which form a monolayered epithelium around the germ line. α-Ada was enriched apically, but could also be detected throughout the basolateral domain in the follicle cells (Fig. 1C,D). At this level of resolution, we observed that some, but not all, apical α-Ada-positive punctae colocalized with Crb (Fig. 1E, arrowhead and arrow, respectively). To confirm that the apical staining of α-Ada is due to expression in follicle cells rather than in germ line cells (oocyte and nurse cells), which are in close contact with the apical surface of follicle cells and also express α-Ada, we generated homozygous $AP\text{-}2\alpha^{3}$ clones in both follicle and/or germ line cells. $AP\text{-}2\alpha^{3}$ is a null allele induced by imprecise excision of a P-element, resulting in the deletion of 5′ non-coding and coding regions, including sequences encoding the N-terminal portion of the protein (González-Gaitán and Jäckle, 1997). α-Ada

Journal of Cell Science (2015) 128, 4538-4549 doi:10.1242/jcs.174573

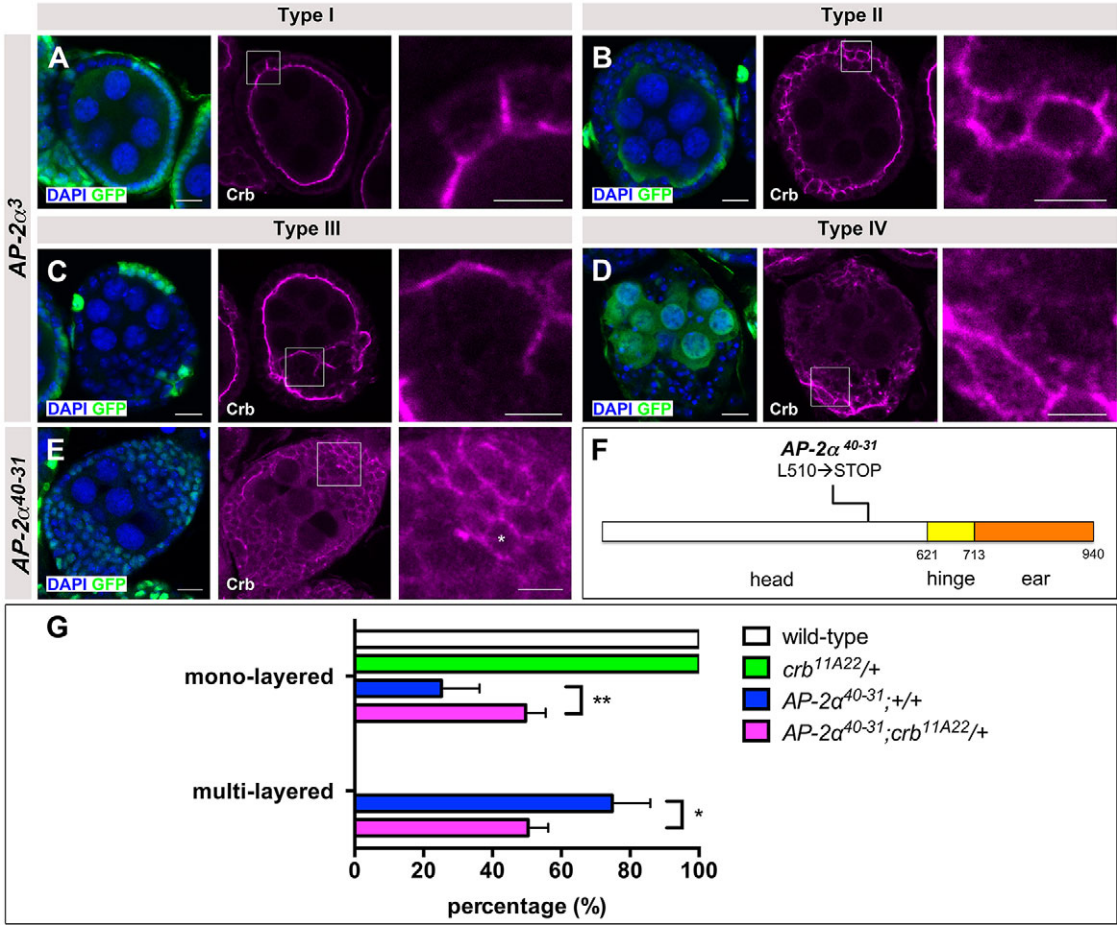

Fig. 2. The AP2 complex is required for the maintenance of epithelial polarity. (A–D) Follicle cells harboring *AP-2α*^{3} clones (lacking GFP), classified into four groups [type I (A), II (B), III (C) and IV (D)] were stained for DAPI (blue) and Crb (magenta). (E) Follicle cells harboring *AP-2α*$^{40\text{-}31}$ clones (labeled with nuclear GFP) stained for DAPI (blue) and Crb (magenta). The asterisk highlights Crb punctae around cell outline. White boxes show the areas that are depicted at higher magnification in the right-hand image. Scale bars: 10 µm (main images); 5 µm (magnified images). (F) Schematic drawing of the molecular characterization of the *AP-2α*$^{40\text{-}31}$ allele. (G) Quantification of the percentage of mutant phenotypes (at stage 2 to stage 8) from three independent experiments. Results are mean±s.d. for n>100 in every experiment. *P<0.05, **P<0.01 (ordinary one-way ANOVA).

staining was still visible at the apical pole of wild-type follicle cells that faced mutant germ line cells. In contrast, when either just follicle cells or follicle and germ line cells were mutant, α-Ada staining was not detected (Fig. S1C,D). This result shows that both α-Ada and Crb are localized apically in cells of the follicular epithelium.

The AP-2 complex regulates Crb localization and levels

To address the functional relationship between α-Ada and Crb, we analyzed the phenotypes of clones homozygous for the loss of function allele *AP-2α*^{3}. Follicular clones for *AP-2α*^{3} showed variable phenotypes, which were classified into four groups according to their severity. Crb expanded laterally in type I follicle cell clones, which did, however, not affect the monolayered organization of the epithelium (Fig. 2A). Cells in type II and III follicular clones were round and formed multi-layered epithelia. Crb was distributed on the whole plasma membranes in type II clones (Fig. 2B), and was partially or completely lost from the plasma membrane in type III clones (Fig. 2C). Cells of type IV follicular clones showed scattered Crb distribution and complete disruption of epithelial polarity and integrity, and often invaded the nurse cells (Fig. 2D). To confirm that these phenotypes were not allele-specific, we generated clones homozygous mutant for other *AP-2α* alleles. Follicular clones mutant for *AP-2α*$^{40\text{-}31}$, an allele that carries a stop codon at the end of the head domain (Fig. 2F), showed punctate staining of Crb surrounding the cell outline and occasional complete loss of Crb, even in cells of the same egg chamber (Fig. 2E). In contrast, *AP-2α*^{ear26} and *AP-2α*^{ear4} did not show any mutant phenotypes when homozygous mutant in follicle cells (Fig. S2B,C). These alleles carry a deletion and a nonsense mutation in the ear domain of α-Ada, respectively (Fig. S2A). The lack of a mutant phenotype might be due to functional redundancy provided by the ear domain of the AP-2β subunit (Owen et al., 1999, 2000; Slepnev and De Camilli, 2000). We also analyzed the phenotypes achieved upon loss of the AP-2σ subunit. Clones mutant for *AP-2σ*^{KG02457}, an allele caused by a P-element insertion in the coding region of the AP-2σ subunit (Bellen et al., 2004; Windler and Bilder, 2010), also showed multi-layering and Crb mislocalization (Fig. S2D).

To analyze whether *AP-2* mutants specifically affect Crb localization, we examined the localization of other polarity proteins in follicle cells. Apical Sdt, PATJ and Par6 were also mislocalized, and their distributions followed that of Crb in *AP-2α*^{3} clones (Fig. S2E–G). Other apically localized proteins, such as the Notch receptor, were also mislocalized and followed the ectopically localized Crb complex (Fig. S2H) (Windler and Bilder, 2010). Concomitant with the expansion of the apical membrane, the Dlg-

Journal of Cell Science (2015) 128, 4538-4549 doi:10.1242/jcs.174573

positive lateral membrane domain was reduced (Fig. S2I). In addition, Armadillo (Arm), the *Drosophila* homologue of vertebrate β-catenin and a marker for the adherens junctions, no longer delineated the adhesion belt, but rather appeared in random spots in regions with epithelial multi-layering (Fig. S2J). These results indicate that disruption of AP-2 function leads to polarity defects.

Strikingly, some of the phenotypes observed upon loss of *AP-2* are similar to those obtained upon Crb overexpression in follicle cells (Fletcher et al., 2012; Tanentzapf et al., 2000). Therefore, we assumed that some of the polarity defects in *AP-2* mutant cells are a consequence of increased and/or mislocalized Crb. If this assumption is correct, removing one copy of *crb* in an *AP-2* homozygous background should reduce the severity of the mutant phenotype. To address this question, we generated homozygous *AP-2α*$^{40\text{-}31}$ follicular clones that carried only one functional copy of *crb* and investigated the percentage of mono- and multi-layered follicular epithelia as indicators of epithelial polarity. Wild-type cells and cells with a single functional copy of *crb* (*crb*^{11A22}/+) formed normal mono-layered epithelia in 100% of all egg chambers analyzed. In contrast, only 25.2% of *AP-2α*$^{40\text{-}31}$ homozygous mutant clones formed mono-layered epithelia. Reducing one copy of *crb* in *AP-2α*$^{40\text{-}31}$ homozygous mutant cells (*AP-2α*$^{40\text{-}31}$; *crb*^{11A22}/+) increased the number of clones forming mono-layered epithelia to 49.6% (Fig. 2G). The data are compatible with the conclusions that at least some aspects of the polarity phenotypes induced by loss of α-Ada are due to mislocalization and/or over-activity of Crb, and that in wild-type cells α-Ada downregulates Crb activity.

We cannot rule out that some defects in Crb distribution observed in *AP-2* mutants might be a secondary consequence due to Crb-independent loss of polarity. To further examine a link between Crb and AP-2, we continued the analysis in imaginal discs because Crb is not required for the maintenance of apico-basal polarity and tissue integrity in these epithelia (Chen et al., 2010; Genevet et al., 2009; Hamaratoglu et al., 2009; Herranz et al., 2006), and the adherens junction marker E-cadherin is still properly localized in *crb* mutant cells (Hafezi et al., 2012; Ribeiro et al., 2014). Unfortunately, most clones mutant for the loss-of-function alleles *AP-2α*^{3} and *AP-2α*$^{40\text{-}31}$ were eliminated from the wing pouch. Cell elimination could be the result of accumulation of JNK-mediated apoptotic signals, or cell competition due to overexpression of Crb (Hafezi et al., 2012). To overcome this problem and study the role of AP-2 in wing discs, we used a transhetero-allelic combination of *AP-2α*$^{40\text{-}31}$ and the temperature-sensitive allele *AP-2α*^{4}. The latter behaves like wild-type when raised at the permissive temperature (18°C), but at restrictive temperatures (i.e. at 25°C and 29°C) its function is partially or fully abolished, respectively (González-Gaitán and Jäckle, 1999). Crb was properly localized at the apical plasma membrane at 18°C, similar to the apical transmembrane protein Stranded at second (Sas) (Fig. 3A,D). At 25°C, no obvious defects were observed, suggesting that a small amount of α-Ada is sufficient for Crb regulation. At 29°C, however, Crb staining appeared in apical punctae and was extended to more lateral regions of the cell (Fig. 3C,F, yellow arrowheads). Interestingly, Sas was still properly localized at the apical membrane under this condition (Fig. 3F), and preliminary results suggest that localization of FasIII on the lateral membrane is not affected. These results suggest that the expansion of the Crb-positive plasma membrane is the result of reduced α-Ada activity, and not due to a general loss of apico-basal polarity. In addition, 69B-Gal4-driven α-Ada knockdown in wing discs led to Crb mislocalization and an increase in Crb levels (Fig. 3G–I). Unlike in wing imaginal discs, large clones homozygous for *AP-2α*$^{40\text{-}31}$ could be obtained in the eye discs. As previously shown, these discs showed strong morphological defects, due to overproliferation and severely disrupted localization of actin and Notch (Windler and Bilder, 2010). In these clones, Crb levels were increased about twofold (Fig. 4B–D). These results suggest that in wild-type cells AP-2 regulates Crb levels.

Internalization of Crb depends on the AP-2 complex

Our results led us to conclude that the AP-2 complex controls Crb levels at the plasma membrane by regulating its internalization. To further substantiate this conclusion, we performed antibody uptake assays in living tissues. However, due to the variable phenotypes developed by *AP-2* mutant follicle cells, consistent conclusions from these results were not possible. As mentioned above, mutant cell clones could not be obtained in wing discs. Moreover, the endocytosis rate of Crb in wild-type imaginal discs was far lower in comparison to Notch (Fig. S3A–F) (Lu and Bilder, 2005). Therefore, we turned to the so-called 'garland' or 'wreath' cells of third-instar larvae. These are nephrocytes forming a garland of cells, which are involved in the segregation and storage of waste products from the hemolymph. They are ideally suited to answer our question: they are big cells (20–30 µm in diameter) that are highly active in endocytosis (Chang et al., 2002; Kosaka and Ikeda, 1983; Soukup et al., 2009; Wigglesworth, 1942) and show endogenous Crb expression on the surface and in cytoplasmic punctate (Fig. S3G,H) (Tepass and Knust, 1990). The anatomical structure and physiological function of garland cells are similar to that of vertebrate podocytes. The plasma membrane of garland cells is compartmentalized, as indicated by the restricted localization of proteins forming the filtration barrier, for example, Sticks and Stones (Sns) and Dumbfounded (Duf), the orthologs of the vertebrate nephrins NPHS1 and NEPH1, respectively (Weavers et al., 2009). When wild-type garland cells were incubated with anti-Crb antibodies, strong surface binding was observed (Fig. 5A), whereas only very faint surface signals were detected upon incubation with an unrelated antibody (data not shown). To monitor Crb internalization in the presence or absence of α-Ada, we performed antibody uptake assays in garland cells from wild-type or *AP-2α*^{3}/*AP-2α*^{4} larvae raised at 29°C, and examined Crb internalization by measuring the fluorescence intensity of Crb from the cell surface to the center of the cell. To quantify the data, we subdivided the distance from the cell surface to the center into three regions (as defined by Kosaka and Ikeda, 1983): (1) the surface region (invagination of plasma membrane and labyrinthine channels, 0–2 µm); (2) the cortical region (2–4 µm), and (3) the cell interior (4–7 µm). At time point 0, Crb was detected on the cell surface within 1 µm, both in wild-type and *AP-2α*^{3}/*AP-2α*^{4} mutants (Fig. 5, 0 min). The rather broad label can be explained by the fact that the plasma membrane of garland cells is highly involuted (Kosaka and Ikeda, 1983; Weavers et al., 2009). After a 5-min chase, the majority of Crb was internalized in wild-type garland cells, and present in vesicles that spread throughout the cell cortex (around 2–3 µm). In contrast, most Crb remained associated with the cell surface (at ~0–2 µm) in *AP-2α*^{3}/*AP-2α*^{4} mutant cells (Fig. 5, 5 min). After a 10-min chase, the intensity on the surface was reduced in wild-type cells and Crb-positive vesicles were apparent in the cytoplasm. In *AP-2α*^{3}/*AP-2α*^{4} mutant cells, some Crb proteins still associated with the surface and only a few vesicles were detected in the cortical region (Fig. 5, 10 min). After a 30-min chase, most staining was gone in wild-type cells, probably due to degradation of Crb. The small amount of Crb proteins observed in

Journal of Cell Science (2015) 128, 4538-4549 doi:10.1242/jcs.174573

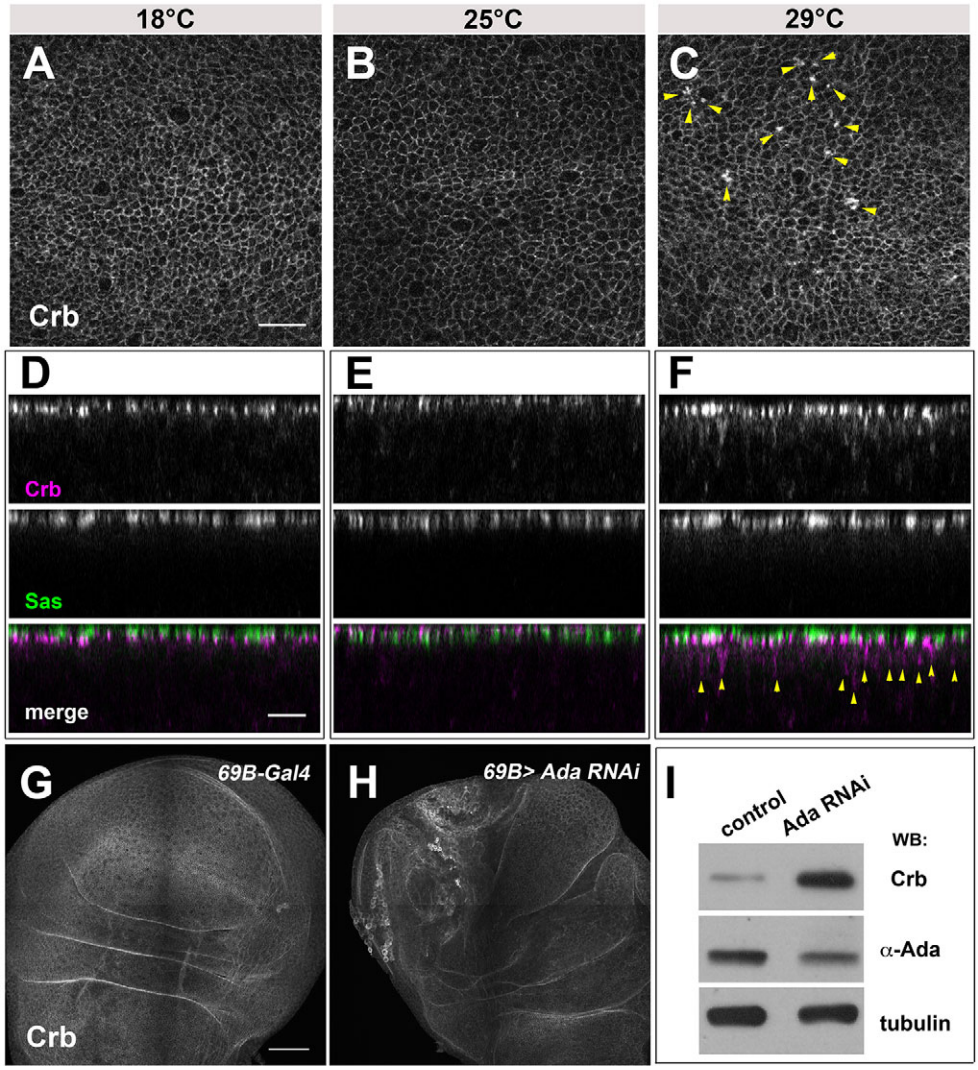

Fig. 3. Crb extends laterally and accumulates upon reduction of α-Ada in wing imaginal discs. (A–F) Wing discs of *AP-2α*$^{40-31}$/*AP-2α*^{4} larvae, raised at 18°C (A,D), 25°C (B,E) and 29°C (C,F) stained for Crb and Sas. Scale bars: 10 µm. (D–F) Single *x-z* sections of wing discs are shown. Crb and Sas appear to be localized at almost the same level of the apical region in most sections analyzed, but, depending on the level of the section, this pattern can occasionally diverge. Scale bars: 5 µm. Yellow arrowheads in C and F highlight expansion of the Crb-positive area. (G,H) RNAi was expressed using 69B-Gal4 drivers. Wing discs were stained for Crb. Scale bar: 50 µm. (I) Western blot from extracts prepared from third-instar wing imaginal discs of 69B-Gal4 (control) and α-Ada-RNAi-expressing flies. Tubulin was used as internal control. Note that α-Ada is reduced, but not completely absent.

some cases on the cell surface may represent recycled proteins (Fig. 5A, 30 min, lower right). In *AP-2α*^{3}/*AP-2α*^{4} mutant cells, Crb-positive punctae were still present in the cell cortex (Fig. 5, 30 min). Residual endocytosis in mutant cells could be explained by the fact that the experimental conditions used (25°C) only resulted in a reduction, but not a complete blockage of AP-2 activity. Taken together, these data clearly demonstrate that α-Ada is required for Crb internalization in garland cells.

The PDZ-binding motif of Crb acts as a sorting signal

Results presented above show that the AP-2 complex is required for Crb internalization, suggesting that Crb is a direct cargo for the

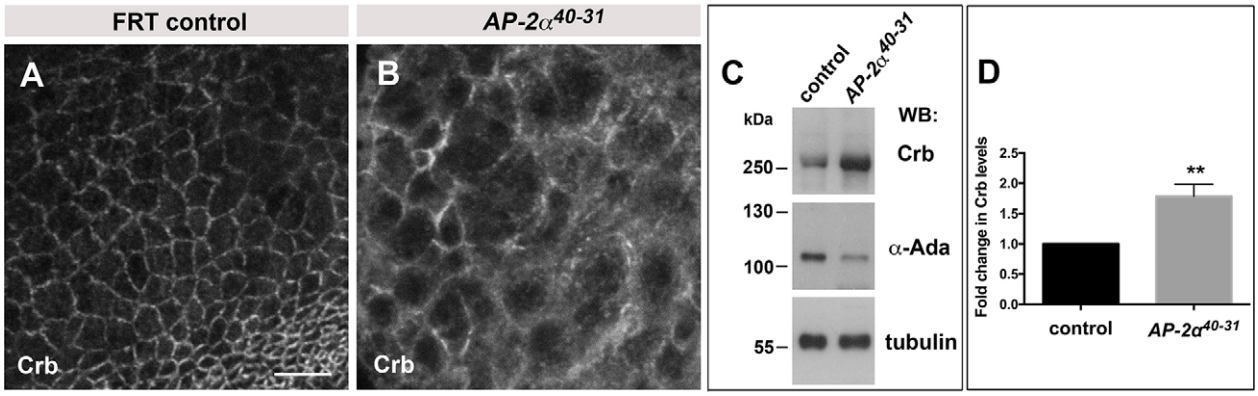

Fig. 4. Crb accumulates in the absence of α-Ada in eye imaginal discs. (A,B) Control and *AP-2α*$^{40-31}$ eye imaginal discs were stained for Crb. Scale bar: 5 µm. (C) Western blot of extracts prepared from *AP-2α*$^{40-31}$ eye imaginal discs. (D) Quantification of western blot results from three independent experiments (mean± s.d.). ***P*<0.01, unpaired *t*-test, one tailed.

Journal of Cell Science (2015) 128, 4538-4549 doi:10.1242/jcs.174573

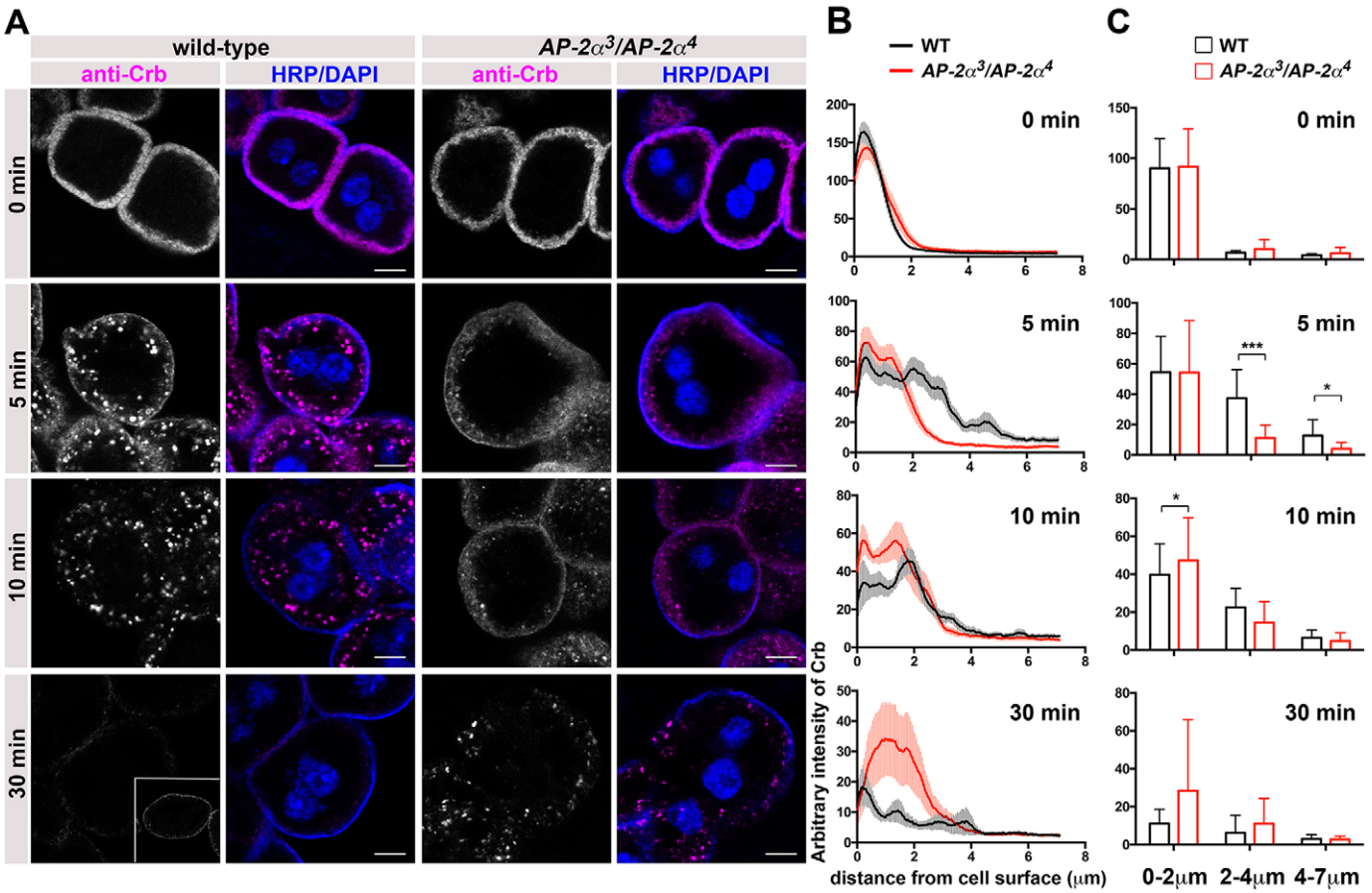

Fig. 5. *AP-2α* mutant garland cells are defective in Crb endocytosis. (A) Antibody uptake assays in garland cells of third-instar larvae. Wild-type or *AP-2α*^{3}/*AP-2α*^{4} garland cells were pulsed with anti-Crb antibodies and chased for the indicated time periods at 25°C. After fixation, garland cells were stained with anti-mouse-IgG secondary antibodies to label Crb (magenta), DAPI (blue) and the membrane marker HRP (blue). The inset in the lower left panel shows a small amount of Crb at the membrane observed in some cases, probably due to recycling. Scale bars: 10 µm. (B) Line-depth intensity plots of anti-Crb antibody staining from the cell surface to cell center in wild-type (black) and *AP-2α*^{3}/*AP-2α*^{4} garland cells (red). Data represent mean±s.e.m., $n \geq 14$ in every genotype. (C) The intensity plot of anti-Crb antibodies, indexed by the distance from cell surface. Bars show mean±s.d., $n \geq 14$ in every genotype. *P<0.05, ***P<0.001 (unpaired *t*-test with Welch's correction).

AP-2 complex. To verify this assumption, we aimed to identify the sorting signal by which Crb is recognized by the AP-2 complex. Several recognition signals in the cytoplasmic tails of transmembrane proteins have been identified. One of them is the di-leucine motif [D/E]xxxL[L/I] (x can be any residue), with L at position 0 and L or I at position +1. The di-leucine motif is typically bordered by polar and/or charged amino acids (reviewed in Pandey, 2009; Traub, 2009). The acidic residue at position −4 (D/E) is only required for targeting to late endosomes or lysosomes, not for internalization (Bonifacino and Traub, 2003). The C-terminal amino acids of the cytoplasmic tail of *Drosophila* Crb (-PPEER**LI**), which is highly conserved in Crb proteins of *Drosophila*, mouse and human (Fig. 1A), fits the di-leucine motif (bold). Strikingly, this motif overlaps with the PDZ-domain-binding motif (underlined), which mediates binding of Sdt or its vertebrate ortholog Pals1 (also known as MPP5) (Bachmann et al., 2001; Hong et al., 2001; Roh et al., 2003). To test whether this motif is required for binding to the AP-2 complex, we generated several mutant versions of the wild-type mCrb2 cytoplasmic tail, fused with a 6×His-TEV-MBP tag (described in Materials and Methods). The mutations either changed or removed the -LI motif, or modified the acidic amino acids EE (Fig. 6A). We confirmed that all mutant versions lacking the C-terminal -LI failed to bind recombinant Pals1, whereas mutations in the acidic amino acids had no effect on binding (Fig. 6B). The interactions between the different Crb versions and AP-2 were tested in liposome recruitment assays as described above. The coupling efficiency of the different mutant proteins to the liposome is documented in Fig. S4. In contrast to the wild-type cytoplasmic domain, all mutant versions tested showed strongly decreased binding to α-Ada (Fig. 6C). This result demonstrates that the PDZ-domain-binding motif of Crb is involved in mediating interactions with the AP-2 complex. The results further indicate that the same motif in the cytoplasmic tail of Crb is required for the interaction with AP-2 and Sdt.

Sdt and AP-2 antagonize to control the surface level of Crb

It is known that *Drosophila* Sdt stabilizes Crb on the apical surface of most epithelia through direct interaction of its PDZ domain with the C-terminus of Crb (Bachmann et al., 2001; Hong et al., 2001; Kempkens et al., 2006). Similarly, vertebrate Pals1 stabilizes Crb1 and Crb3 on the plasma membrane of photoreceptor cells and Madin-Darbine canine kidney (MDCK) epithelial cells in culture (Makarova et al., 2003; Park et al., 2011; Roh et al., 2003; van Rossum et al., 2006). Here, we showed that both Pals1 and the AP-2 complex require the same region of mCrb2 for interaction (Fig. 6B,C). We therefore asked whether this has any biological

Journal of Cell Science (2015) 128, 4538-4549 doi:10.1242/jcs.174573

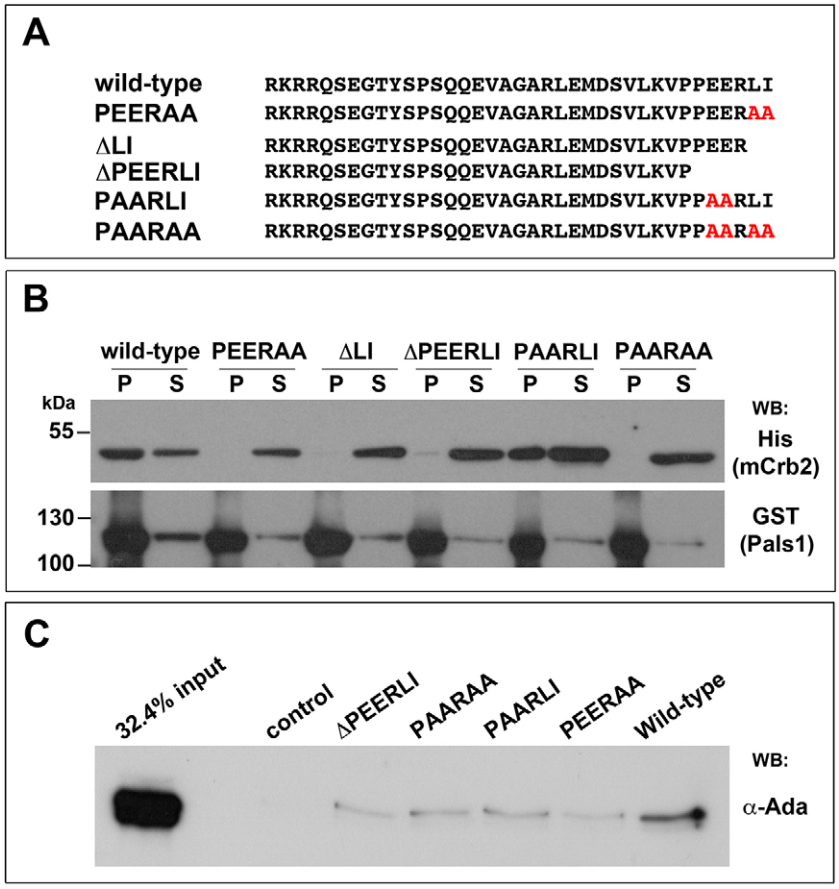

Fig. 6. The cytoplasmic tails of Crb directly interact with the AP-2 complex. (A) Amino acid sequences of the cytoplasmic tails of mCrb2 variants used in this study. Altered amino acids are indicated in red. (B) Western blot of a GST pulldown assay using different forms of 6×His-TEV-MBP-mCrb2 (the molecular mass is ~55 kDa) and GST–Pals1. P, pellet fraction; S, unbound fraction. (C) Western blot of proteins eluted from mCrb2 liposome recruitment assays, probed for α-Ada.

significance *in vivo*. Given the high degree of conservation between mCrb2 and Pals1 and *Drosophila* Crb and Sdt, we studied Crb expression in the *Drosophila* wing discs upon knockdown of *sdt* alone or *sdt* together with *AP-2α*. Knockdown was achieved by RNAi expression in the posterior compartment of the larval wing discs using *engrailed*-Gal4. Both Crb and Sdt were localized apically in the anterior and posterior compartment of the wing pouch in control discs when *engrailed*-Gal4 was expressed alone (Fig. 7A). Overexpression of *AP-2α* RNAi was performed under conditions that only mildly reduced *AP-2α* in order to get a sensitized background. Under these conditions, neither Crb nor Sdt levels differed from that of wild-type control discs (compare Fig. 7A and 7B), probably due to the fact that a small amount of α-Ada is sufficient. As expected, knocking down Sdt resulted in a reduction of Crb at the apical surface (Fig. 7C,E,F). Strikingly, when both *sdt* and *AP-2α* were knocked down simultaneously, cells showed wild-type levels of Crb on the surface (Fig. 7D–F). These data suggest that the presence of Sdt prevents *AP-2α*-dependent Crb internalization and degradation in the wing-disc epithelium.

DISCUSSION

Data presented here, obtained using genetic and biochemical assays, led us to conclude that a delicate balance of stabilization and internalization controls proper Crb levels at the surface. This balance is mediated by binding of a conserved amino acid sequence of Crb to either Sdt or AP-2, suggesting a competitive binding between Sdt and AP-2. Such a mechanism, based on stabilization by PDZ–ligand interaction and AP-2-mediated endocytosis, has so far only been described for a few proteins, such as the NR2B subunit of the neuronal NMDA receptor (Prybylowski et al., 2005) and the glutamate transporter excitatory amino acid carrier 1 (EAAC1) in MDCK cells. In the latter case, AP-2 and the PDZ domain of PDZK1 antagonistically regulate surface levels of EEAC1 by binding to two closely adjacent binding sites in EEAC1 (D'Amico et al., 2010).

Currently, we can only speculate about the mechanisms that might determine which of the binding partners – AP-2 or Sdt – binds to Crb. One possibility is that different binding affinities between Crb and its partners modulate the binding preference. Several arguments suggest that binding of AP-2 to Crb seems to be weaker than the Sdt–Crb interaction. First, AP-2–Crb interactions could only be shown by liposome recruitment assays, but not by standard pulldown experiments (data not shown), suggesting that the presence of membranes strengthen the interaction between the adaptor and its cargo. In fact, interaction of AP-2 with phosphatidylinositol 4,5-bisphosphate [PtdIns(4,5)P_2]-containing membranes induces a conformational change of the AP-2 complex, thus facilitating binding to its cargo (Jackson et al., 2010; Kelly et al., 2008). Second, binding of Sdt only depends on the C-terminal leucine and isoleucine residues of Crb. This is in agreement with recently published structural data using crystallography and fluorescence polarization, which show that the four C-terminal amino acids of human Crb1 interact with the PDZ domain of Pals1 by van der Waals contacts and charged interactions (Ivanova et al., 2015). In contrast, AP-2 binding to Crb requires the glutamine and arginine residues of Crb as well as the leucine and isoleucine residues, at least under the *in vitro* conditions used here. The importance of more than one motif for strong binding of AP-2 is not unprecedented. Binding of the human immunodeficiency (HIV)-1 protein Nef to the α–σ2-hemicomplex of AP-2 requires both a di-

Journal of Cell Science (2015) 128, 4538-4549 doi:10.1242/jcs.174573

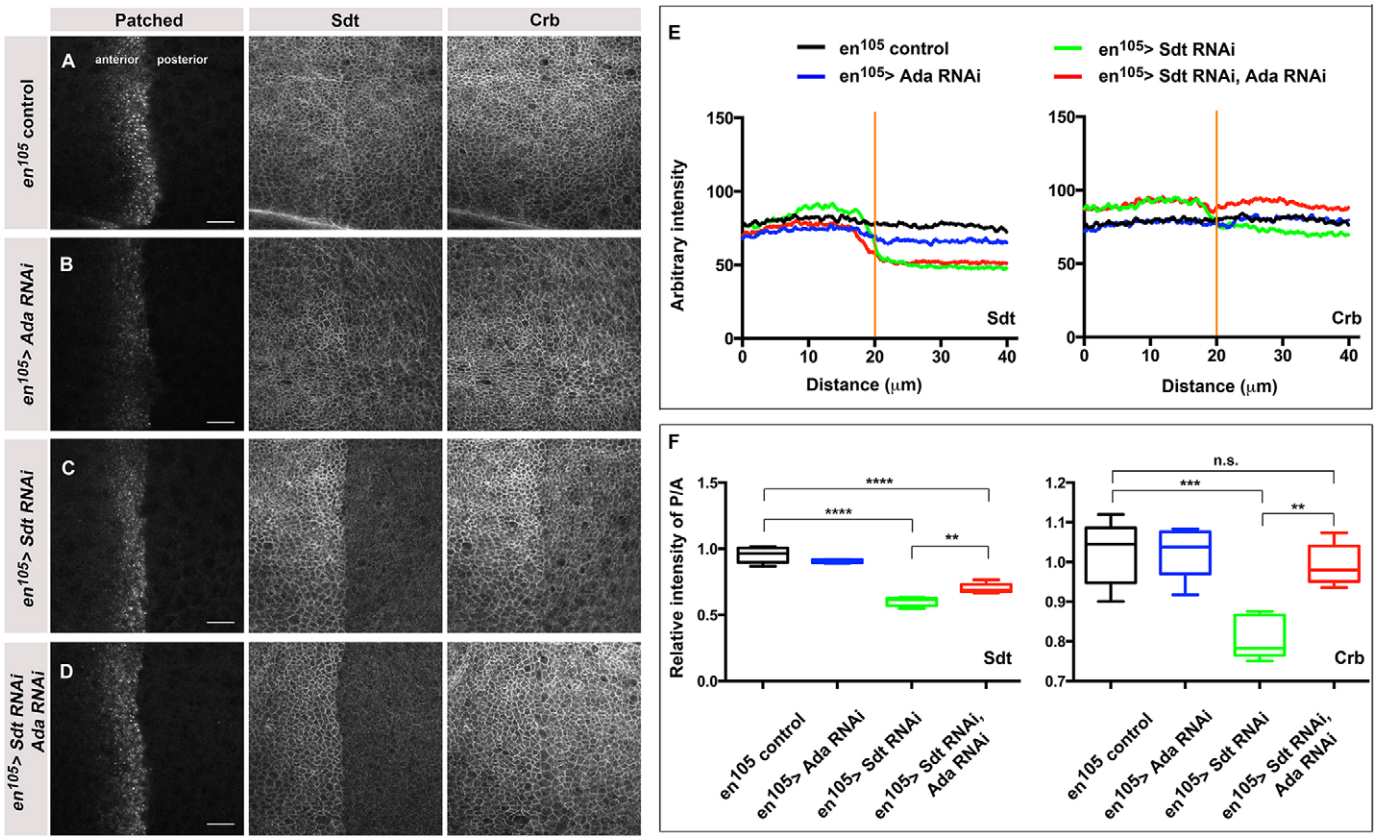

Fig. 7. Antagonistic activities of Sdt and the AP-2 complex to stabilize Crb on the plasma membrane. (A–D) RNAi was expressed in the posterior compartment using *engrailed*^{105}-Gal4. Third-instar wing imaginal discs were stained for Patched (Ptc), to label the anterior–posterior compartment boundary, Sdt and Crb. The *x-y* views show apical confocal projections corresponding to 2.6 µm. Scale bars: 10 µm. (E) Quantification of Sdt and Crb intensity, plotted along the anterior–posterior axis. The orange line marks the anterior–posterior boundary. Data show the mean, *n*=5. (F) Box plot of relative intensity of the posterior to anterior intensity ratio (P/A) of Sdt and Crb. The box represents the 25–75th percentiles, and the median is indicated. The whiskers represent 1.5 of the interquartile range. *n*=5. ***P*<0.01, ****P*<0.001, *****P*<0.0001 (ordinary one-way ANOVA).

leucine- and a di-acidic-motif (Craig et al., 1998; Lindwasser et al., 2008). Posttranslational modification of the ligand Crb itself could also contribute to a preferred binding to either Sdt/Pals1 or AP-2. It has recently been documented that aPKC-mediated phosphorylation of threonine residues near the FBM of Crb abolishes the Crb–Moesin interaction, but not the Crb–Pals1 interaction (Wei et al., 2015). In the case of *Drosophila* Gliotactin, a transmembrane protein at the tricellular junction, phosphorylation of tyrosine residues is necessary for its endocytosis and ultimately lysosomal degradation, thus preventing overexpression, which would result in delamination, migration and finally apoptosis of cells (Padash-Barmchi et al., 2010). Alternatively, the accessibility of the PDZ domain of Sdt/Pals1 to Crb could be modulated. In fact, a ∼100-fold stronger binding of the PDZ domain of Pals1 to the Crb tail is achieved upon intra- or inter-molecular interactions between the Src homology 3 (SH3)- and the guanylate kinase (GUK)-domain of Pals1 (Kantardzhieva et al., 2005; Li et al., 2014). Similarly, the affinity of the PDZ domain of the postsynaptic density protein PSD-95 to its ligand is reduced upon phosphorylation of a tyrosine residue in a linker region between the third PDZ domain and the subsequent SH3-domain, thereby weakening the intramolecular interaction between the PDZ and the SH3 domain (Murciano-Calles et al., 2014; Zhang et al., 2011).

A striking observation was the high degree of phenotypic variability upon knockdown and knockout of AP-2 in different epithelial tissues, and sometimes even in the same epithelium. This prevented us from studying the different aspects of the AP-2–Crb relationship in just one epithelium. In the follicle epithelium, the phenotypes ranged from minor expansion of the apical surface to complete loss of polarity and overgrowth. Complete loss of *AP-2α* in wing discs led to cell lethality, whereas mutant clones survived in eye discs. This variability might be due to the time point of induction of mitotic recombination, which could occur before or after establishment of epithelial polarity, or at time points of high or low Crb expression (Sherrard and Fehon, 2015). Alternatively, additional AP-2-independent polarity regulators could act redundantly and in a tissue- and/or time-specific manner, thus modulating the severity of the phenotype, for example, in the developing eye.

The results described here are compatible with the assumption that several phenotypes obtained by loss or reduction of *AP-2* are a consequence of increased Crb levels on the plasma membrane, given that similar phenotypes can be obtained upon overexpression of Crb (Fletcher et al., 2012; Kempkens et al., 2006; Klebes and Knust, 2000; Laprise et al., 2006; Lu and Bilder, 2005; Pellikka et al., 2002; Tanentzapf et al., 2000; Wodarz et al., 1995). First, the Crb-positive plasma membrane in *AP-2α* mutants cells is expanded both in the imaginal discs and the follicle epithelium, often at the expense of the lateral membrane. Second, without functional *AP-2α*, the monolayered epithelium is often disrupted and becomes multilayered. Third, surviving *AP-2α*^{3} clones in eye imaginal discs show strong Crb enrichment, similar to that in HEK293 cells in

Journal of Cell Science (2015) 128, 4538-4549 doi:10.1242/jcs.174573

which *AP-2α* is knocked down by RNAi (data not shown). Fourth, assuming that a similar increase in Crb also occurs in *AP-2α*^{3} mutant cells induced in wing discs, their elimination could be a consequence of cell competition when next to wild-type cells as recently described (Hafezi et al., 2012). Finally, the multi-layering phenotype of follicle epithelia lacking *AP-2α* can be partially suppressed by removing one copy of *crb*.

A more direct insight into the relationship between Crb and AP-2 comes from our analysis of the garland cells, the functional equivalent of vertebrate podocytes. Podocytes are highly specialized epithelial cells in the kidney of vertebrates, which form long 'foot-processes' connected by slit diaphragms to form a filtration barrier in the renal glomerula. Interestingly, Crb2 is expressed in the kidney of both rats and zebrafish, where it localizes at the slit diaphragm of podocytes. *crb2b* mutant zebrafish show defects in the formation of the slit diaphragm as well as in arborization of the foot processes. Furthermore, mutations in human *Crb2* are linked to steroid-resistant nephrotic syndrome (Ebarasi et al., 2015), a disease causing kidney failure due to defects in differentiation and function of podocytes. Here, we show that *AP-2α* mutant garland cells are clearly impaired in Crb endocytosis. Whether loss of *crb* in garland cells affects their excretory function should be determined.

A complex machinery is required to ensure proper Crb surface levels, which is key for the maintenance of apico-basal epithelial cell polarity. Crb levels can be regulated at multiple levels, including stabilization at the membrane through homophilic interactions of the extracellular domains in cis or trans, interactions of the cytoplasmic tail with scaffolding proteins, endocytosis, degradation and recycling by the retromer. The trafficking pathway offers multiple steps for regulation, and results presented here provide further mechanistic insight into how binding of two counteracting PDZ-motif-binding proteins, Sdt and AP-2, regulate proper Crb levels. Given the finding that the balance between Crb stabilization and its internalization and degradation is crucial for surface expression of Crb and hence polarity, future work will aim to identify the mechanisms that control this balance by regulating the rate of endocytosis, degradation and recycling by the retromer. Finding these regulators is challenging, but will give us important insights into the mechanisms coordinating endocytosis and polarity, which is important to prevent tumorigenesis not only in *Drosophila*, but also in vertebrates.

MATERIALS AND METHODS

Genetics

All flies were raised at 25°C unless otherwise indicated. Clones in the follicular epithelium were generated by Flippase driven by a heat-shock promoter to induce mitotic recombination (Xu and Rubin, 1993). Clones were marked either positively (MARCM) or negatively (lacking GFP), using *yw-hsFLP tub-Gal4 UAS-nls-GFP; FRT40A tub-Gal80* [a gift from Thomas Klein, Institute of Genetics, University of Duesseldorf, Germany (Kaspar et al., 2008)] or *yw-hsFLP; FRT40A ubi-GFP* (a gift from Christian Dahmann, Department of Systems Biology and Genetics, Institute of Genetics of the Technical University Dresden, Germany). Heat shock was performed on third-instar larvae at 37°C for 1.5 or 2 h on a consecutive two days. *FRT40A AP-2α*^{3}, *AP-2α*^{ear4} and *AP-2α* ^{ear26} were gifts from Jürgen Knoblich, Institute of Molecular Biotechnology GmbH, Austria (Berdnik et al., 2002). *FRT40A AP-2α* $^{40-31}$ was a gift from David Bilder, Cell and Molecular Biology, University of California Berkeley, USA (Windler and Bilder, 2010). *FRT82B AP2σ*^{KG02457} was a gift from Bingwei Lu, Department of Pathology, Stanford University School of Medicine, USA (Song and Lu, 2012). *AP-2α*^{4} was a gift from Marcos González-Gaitán, Biochemistry Department, University of Geneva, Switzerland (González-Gaitán and Jäckle, 1999). *engrailed*^{105}*-Gal4* and *69B-Gal4* were gifts from Suzanne Eaton, MPI for Molecular Cell Biology and Genetics Dresden, Germany (Eugster et al., 2007). *UAS Ada RNAi* (VDRC #15565 and #15566) and *UAS Sdt RNAi* (Bloomington #37510) were purchased from the Vienna *Drosophila* RNAi center (VDRC) and Bloomington Stock Center, respectively. To obtain *AP-2α* trans-heterozygous mutant in wing discs, crosses were raised at 18°C to overcome embryonic lethality and temperature shifts were performed at the second larval instar. Discs were dissected 2 days later after the temperature shift. Large clones of *AP-2α* mutants in eye disc were obtained by crossing males mutant for *AP-2α*$^{40-31}$ to virgins carrying a cell lethal mutation on an FRT chromosome (Bloomington stock #5622).

Antibodies

The following primary antibodies were used in this study at the concentration indicated: rabbit anti-α-Ada (1:50, immunofluorescence, a gift from Marcos González-Gaitán), mouse anti-Arm (1:1000, immunofluorescence, DSHB), rat anti-Crb 2.8 (1:1000, immunofluorescence, 1:2000, western blotting; Tepass and Knust, 1990), rat anti-Crb exon 3 (1:1000, immunofluorescence, unpublished), mouse anti-Crb Cq4 (1:200, western blotting; Tepass and Knust, 1993), mouse anti-Dlg 4F3 (1:1000, immunofluorescence; DSHB), rabbit anti-PATJ (1:1000, immunofluorescence, 1:4000, western blotting; Richard et al., 2006), mouse anti-Notch C458.2H (1:1000, immunofluorescence; DSHB), guinea pig anti-Par6 (1:1000, immunofluorescence; kindly provided by Andreas Wodarz, Institute of Anatomy, University of Cologne, Germany), mouse anti-Patched (1:200, immunofluorescence; DSHB), rabbit anti-Sdt (1:1000, immunofluorescence, 1:5000, western blotting, Berger et al., 2007), rabbit anti-Sas (1:1000, immunofluorescence, a gift from Douglas Cavener, Department of Biology, Pennsylvania University, USA), mouse anti-α-Ada (1:1000, western blotting; Santa Cruz Biotechnology), rabbit anti-γ-adaptin 1 (1:500, western blotting; Santa Cruz Biotechnology), rat anti-tubulin (1:5000, western blotting; AbD Serotec), rabbit anti-GFP (1:2000, immunofluorescence; Invitrogen), and normal anti-rabbit-IgG (Santa Cruz Biotechnology) antibodies. Fluorescence-conjugated secondary antibodies were purchased from Invitrogen (1:1000, immunofluorescence). Horseradish peroxidase (HRP)-labeled secondary antibodies were against rat (1:3000, western blotting; Dianova), rabbit and mouse (1:3000, western blotting; Sigma) IgG. Rat polyclonal anti-α-Ada serum (1:2000, western blotting) was generated as previously described (González-Gaitán and Jäckle, 1997). Briefly, rats were immunized and boosted with His-tagged *Drosophila* α-Ada C-terminal region (amino acids 580–940) in combination with complete or incomplete Freund's adjuvants (Charles River). Serum from the final bleed was clarified by centrifugation.

Protein extraction and western blot

Imaginal discs were lysed in 2× SDS loading buffer (0.02% Bromophenol Blue, 2% SDS, 125 mM Tris-HCl pH 6.8, 3.3% glycerol, 6% β-mercaptoethanol, 200 mM dithiothreitol) and homogenized. Samples were boiled at 95°C for 5 min, clarified by centrifugation at 20,000 ***g*** for 10 min. Proteins were separated by SDS-PAGE, transferred onto Nitrocellulose filters (GE Healthcare) and blocked in 1% bovine serum albumin (BSA) in Tris-buffered saline with Triton X-100 (TBST; 0.2% Triton X-100). Antibodies were used as described above.

Immunofluorescence staining and confocal microscopy

Drosophila ovaries, imaginal discs and garland cells were fixed in 4% PFA for 20 min. For α-Ada staining of follicle cells, ovaries were fixed in 4% PFA in PBST (0.15% Triton X-100) for 20 min. Ovaries were further fixed in 100% ethanol at −20°C overnight and then permeabilized with PBST (0.5% Triton X-100), followed by blocking in 5% BSA. Imaginal discs and garland cells were washed with PBST (0.1% Triton X-100) and blocked in 0.1% BSA. *Drosophila* tissues were incubated with primary antibodies at 4°C overnight. After washing, fluorescence-conjugated secondary antibodies were added for 2 h at room temperature and mounted in ProlongGold antifade reagent (Invitrogen). For surface staining of garland cells, all procedures were the same except that detergents were

omitted. All images were acquired by using Zeiss LSM700 (Zeiss Plan-Neofluar 25× NA 0.8 or Zeiss LCI Plan-Neofluar 63× NA 1.3 objective; the immersion medium was 50% glycerol) and processed by Fiji and Adobe Photoshop.

DNA constructs and site-directed mutagenesis

The mCrb2 tail construct (pET28-6X His-MBP-TEV-mCrb2) was made as previously published (Pocha et al., 2011). To make mCrb2 tail mutants, the QuikChange site-directed mutagenesis kit (Stratagene) was used with the wild-type construct as a template. Human Pals1 was cloned into pGEX4T-2 (GE Healthcare) using BamHI and NotI restriction sites.

Antibody uptake assay

Uptake assays in garland cells were performed and modified as described previously (Kim et al., 2010; Weavers et al., 2009). Garland cells of third-instar larvae were dissected in cold PBS and pulsed with purified mouse monoclonal anti-Crb exon 3 antibodies (200 µg/ml) at 4°C for 15 min. After washing off unbound antibodies, garland cells were chased for the indicated time periods at room temperature in PBS. Samples were fixed in 4% PFA for 20 min, washed in PBS, and incubated with rabbit anti-HRP antibody (1:500, immunofluorescence; Jackson ImmunoResearch Laboratories) for 2 h to mark the plasma membrane (Soukup et al., 2009). Samples were washed in PBST (0.05% Triton X-100), blocked with 0.1% BSA, incubated with fluorescent-tag-conjugated secondary antibodies for 2 h, and mounted in ProlongGold antifade reagent (Invitrogen). Garland cells were identified by the presence of two nuclei (Kosaka and Ikeda, 1983) and HRP-positive staining. Antibody uptake assay in wing discs were performed and modified as previously described (Le Borgne et al., 2005; Lu and Bilder, 2005). Briefly, wing discs were dissected in Grace's insect medium (Sigma #G8142) and were cut between the hinge region and the wing pouch to facilitate antibody diffusion. Wing discs were pulsed with mouse anti-Notch C458.2H (10 µg/ml) or mouse anti-Crb exon 3 antibodies (200 µg/ml) at 4°C for 2 h, and then cultured in Grace's insect medium supplemented with 1% fetal bovine serum for the indicated time. Wing discs were fixed and permeabilized followed by secondary antibody staining.

Image analysis and quantification

The line-plot density profile for the antibody uptake assay was generated as previously described (Kim et al., 2010). Briefly, a line intensity profile (100 px, 5 µm) was measured from the cell surface to the cell center by Fiji. For establishing the intensity profile in wing discs, the fluorescence intensity was quantified within the same size of the box along the anterior–posterior axis. For determination of the posterior to anterior intensity ratio, the average fluorescence intensity in the posterior compartment within the box was divided by the average in the anterior compartment. All charts were made with Graphpad Prism 6. Statistical analysis was undertaken with Graphpad Prism 6. Western blots were analyzed by Fiji software.

Protein expression and purification

6×His-MBP-TEV-mCrb2 tail and GST-Pals1 were expressed in *E. coli* strain BL21 pLysS (DE3) and purified using Ni-NTA (Qiagen) and glutathione–Sepharose (GE Healthcare), respectively, according to the manufacturers' instruction. mCrb2 tail proteins were eluted with 250 mM imidazole and dialyzed for further assay (20 mM HEPES pH 7.2, 125 mM potassium acetate and 1 mM EDTA). GST fusion proteins were eluted with 10 mM reduced glutathione and dialyzed (10 mM Tris-HCl pH 8.0, 150 mM NaCl).

Purification of mixed adaptors and proteo-liposome recruitment assay

Mixed adaptors were purified from clathrin-coated vesicles isolated from pig brain, essentially as described previously (Keen, 1987). Mixed adaptors were isolated from a Tris-HCl extract of clathrin-coated vesicles by gel filtration, using Sephacryl S-500. The adaptor-containing fractions were concentrated using saturated ammonium sulphate precipitation, and were dialyzed into, and stored in, 1 M Tris buffer (0.05 M Tris base, 0.95 M Tris-HCl, 1 mM EDTA, 0.1% β-mercaptoethanol and 0.02% sodium azide). Proteo-liposome recruitment assays were performed essentially as described previously (Pocha et al., 2011) with the following modifications. The liposomes used in this study were made up of phosphatidylcholine (Sigma-Aldrich), phosphatidylethanolamine (Sigma-Aldrich), phosphatidylserine (Sigma-Aldrich), cholesterol (Sigma-Aldrich) and 1,2-dioleoyl-*sn*-glycero-3-phosphoethanolamine-N-[4-(p-maleimidomethyl)cyclohexane-carboxamide] (sodium salt; Avanti Polar Lipids; molar ratio: 40:30:10:10:10). Dialyzed mCrb2 tail proteins were digested by TEV protease and coupled to the liposomes. mCrb2-tail-conjugated liposomes were incubated in 25 µg of purified mixed adaptors for 30 min at 37°C, and then isolated by centrifugation using a sucrose cushion composed of 3 ml 60% sucrose, followed by 8 ml of 5% sucrose in recruitment buffer (20 mM HEPES pH 7.2, 125 mM potassium acetate and 2.5 mM magnesium acetate). Liposomes were harvested from the interface between the two sucrose amounts, and pelleted by ultracentrifugation (100,000 ***g***). The pelleted liposomes were re-suspended and subjected to analysis by SDS-PAGE and western blotting.

Pulldown assay

Recombinant GST–Pals1 and His-MBP–mCrb2 tails were incubated in the binding buffer (20 mM HEPES, pH 7.2, 150 mM NaCl, 1 mM $MgCl_2$ and 0.1% Triton X-100) at 4°C, rotated for 1.5 h, before addition of glutathione–Sepharose (GE Healthcare) and a further 2 h of rotation. The beads were washed and boiled at 95°C in SDS-loading buffer for 5 min. Samples were analyzed by SDS-PAGE and western blotting.

Acknowledgements

We are grateful to Marino Zerial, Sarita Hebbar and Linda Nemetschke for critical reading of the manuscript. We also thank the Protein Expression and Purification Facility, the Antibody Facility and the Light Microscopy Facility at MPI-CBG for technical assistance. We thank the Bloomington *Drosophila* Stock Center and Vienna *Drosophila* RNAi center for fly stocks and the Developmental Studies Hybridoma Bank for antibodies.

Competing interests

The authors declare no competing or financial interests.

Author contributions

Y.-H.L., H.C., S.M.P. and A.R. carried out experiments, Y.-H.L., T.W. and E. K. designed experiments and contributed to data analysis, and Y.-H.L. and E.K. wrote the manuscript. All authors reviewed the manuscript prior to submission.

Funding

We acknowledge funding from the Max-Planck Society to E. K.; and from the Biotechnology and Biomedical Sciences Research Council [grant number BB/K014862/1 to T.W.]. Y.-H.L. was supported by the Dresden International Graduate School for Biomedicine and Bioengineering (DIGS-BB).

Supplementary information

Supplementary information available online at
http://jcs.biologists.org/lookup/suppl/doi:10.1242/jcs.174573/-/DC1

References

Bachmann, A., Schneider, M., Theilenberg, E., Grawe, F. and Knust, E. (2001). *Drosophila* Stardust is a partner of Crumbs in the control of epithelial cell polarity. *Nature* **414**, 638-643.

Baust, T., Czupalla, C., Krause, E., Bourel-Bonnet, L. and Hoflack, B. (2006). Proteomic analysis of adaptor protein 1A coats selectively assembled on liposomes. *Proc. Natl. Acad. Sci. USA* **103**, 3159-3164.

Bellen, H. J., Levis, R. W., Liao, G., He, Y., Carlson, J. W., Tsang, G., Evans-Holm, M., Hiesinger, P. R., Schulze, K. L., Rubin, G. M. et al. (2004). The BDGP gene disruption project: single transposon insertions associated with 40% of *Drosophila* genes. *Genetics* **167**, 761-781.

Berdnik, D., Török, T., González-Gaitán, M. and Knoblich, J. A. (2002). The endocytic protein alpha-Adaptin is required for numb-mediated asymmetric cell division in *Drosophila*. *Dev. Cell* **3**, 221-231.

Berger, S., Bulgakova, N. A., Grawe, F., Johnson, K. and Knust, E. (2007). Unraveling the genetic complexity of *Drosophila stardust* during photoreceptor morphogenesis and prevention of light-induced degeneration. *Genetics* **176**, 2189-2200.

Boehm, M. and Bonifacino, J. S. (2001). Adaptins: the final recount. *Mol. Biol. Cell* **12**, 2907-2920.
Bonifacino, J. S. and Traub, L. M. (2003). Signals for sorting of transmembrane proteins to endosomes and lysosomes. *Annu. Rev. Biochem.* **72**, 395-447.
Bulgakova, N. A. and Knust, E. (2009). The Crumbs complex: from epithelial-cell polarity to retinal degeneration. *J. Cell Sci.* **122**, 2587-2596.
Chang, H. C., Newmyer, S. L., Hull, M. J., Ebersold, M., Schmid, S. L. and Mellman, I. (2002). Hsc70 is required for endocytosis and clathrin function in *Drosophila*. *J. Cell Biol.* **159**, 477-487.
Chen, C.-L., Gajewski, K. M., Hamaratoglu, F., Bossuyt, W., Sansores-Garcia, L., Tao, C. and Halder, G. (2010). The apical-basal cell polarity determinant Crumbs regulates Hippo signaling in *Drosophila*. *Proc. Natl. Acad. Sci. USA* **107**, 15810-15815.
Craig, H. M., Pandori, M. W. and Guatelli, J. C. (1998). Interaction of HIV-1 Nef with the cellular dileucine-based sorting pathway is required for CD4 down-regulation and optimal viral infectivity. *Proc. Natl. Acad. Sci. USA* **95**, 11229-11234.
Crottet, P., Meyer, D. M., Rohrer, J. and Spiess, M. (2002). ARF1·GTP, tyrosine-based signals, and phosphatidylinositol 4,5-bisphosphate constitute a minimal machinery to recruit the AP-1 clathrin adaptor to membranes. *Mol. Biol. Cell* **13**, 3672-3682.
D'Amico, A., Soragna, A., Di Cairano, E., Panzeri, N., Anzai, N., Vellea Sacchi, F. and Perego, C. (2010). The surface density of the glutamate transporter EAAC1 is controlled by interactions with PDZK1 and AP2 adaptor complexes. *Traffic* **11**, 1455-1470.
de Vreede, G., Schoenfeld, J. D., Windler, S. L., Morrison, H., Lu, H. and Bilder, D. (2014). The Scribble module regulates retromer-dependent endocytic trafficking during epithelial polarization. *Development* **141**, 2796-2802.
Ebarasi, L., Ashraf, S., Bierzynska, A., Gee, H. Y., McCarthy, H. J., Lovric, S., Sadowski, C. E., Pabst, W., Vega-Warner, V., Fang, H. et al. (2015). Defects of CRB2 cause steroid-resistant nephrotic syndrome. *Am. J. Hum. Genet.* **96**, 153-161.
Eugster, C., Panáková, D., Mahmoud, A. and Eaton, S. (2007). Lipoprotein-heparan sulfate interactions in the Hh pathway. *Dev. Cell* **13**, 57-71.
Fletcher, G. C., Lucas, E. P., Brain, R., Tournier, A. and Thompson, B. J. (2012). Positive feedback and mutual antagonism combine to polarize Crumbs in the *Drosophila* follicle cell epithelium. *Curr. Biol.* **22**, 1116-1122.
Genevet, A., Polesello, C., Blight, K., Robertson, F., Collinson, L. M., Pichaud, F. and Tapon, N. (2009). The Hippo pathway regulates apical-domain size independently of its growth-control function. *J. Cell Sci.* **122**, 2360-2370.
Godlee, C. and Kaksonen, M. (2013). Review series: from uncertain beginnings: initiation mechanisms of clathrin-mediated endocytosis. *J. Cell Biol.* **203**, 717-725.
González-Gaitán, M. and Jäckle, H. (1997). Role of *Drosophila* α-adaptin in presynaptic vesicle recycling. *Cell* **88**, 767-776.
González-Gaitán, M. and Jäckle, H. (1999). The range of spalt-activating Dpp signalling is reduced in endocytosis-defective *Drosophila* wing discs. *Mech. Dev.* **87**, 143-151.
Grawe, F., Wodarz, A., Lee, B., Knust, E. and Skaer, H. (1996). The *Drosophila* genes *crumbs* and *stardust* are involved in the biogenesis of adherens junctions. *Development* **122**, 951-959.
Hafezi, Y., Bosch, J. A. and Hariharan, I. K. (2012). Differences in levels of the transmembrane protein Crumbs can influence cell survival at clonal boundaries. *Dev. Biol.* **368**, 358-369.
Hamaratoglu, F., Gajewski, K., Sansores-Garcia, L., Morrison, C., Tao, C. and Halder, G. (2009). The Hippo tumor-suppressor pathway regulates apical-domain size in parallel to tissue growth. *J. Cell Sci.* **122**, 2351-2359.
Harris, K. P. and Tepass, U. (2008). Cdc42 and Par proteins stabilize dynamic adherens junctions in the *Drosophila* neuroectoderm through regulation of apical endocytosis. *J. Cell Biol.* **183**, 1129-1143.
Herranz, H., Stamataki, E., Feiguin, F. and Milán, M. (2006). Self-refinement of Notch activity through the transmembrane protein Crumbs: modulation of γ-secretase activity. *EMBO Rep.* **7**, 297-302.
Hong, Y., Stronach, B., Perrimon, N., Jan, L. Y. and Jan, Y. N. (2001). *Drosophila* Stardust interacts with Crumbs to control polarity of epithelia but not neuroblasts. *Nature* **414**, 634-638.
Ivanova, M. E., Fletcher, G. C., O'Reilly, N., Purkiss, A. G., Thompson, B. J. and McDonald, N. Q. (2015). Structures of the human Pals1 PDZ domain with and without ligand suggest gated access of Crb to the PDZ peptide-binding groove. *Acta Crystallogr. D Biol. Crystallogr.* **71**, 555-564.
Jackson, L. P., Kelly, B. T., McCoy, A. J., Gaffry, T., James, L. C., Collins, B. M., Höning, S., Evans, P. R. and Owen, D. J. (2010). A large-scale conformational change couples membrane recruitment to cargo binding in the AP2 clathrin adaptor complex. *Cell* **141**, 1220-1229.
Jürgens, G., Wieschaus, E., Nüsslein-Volhard, C. and Kluding, H. (1984). Mutations affecting the pattern of the larval cuticle of *Drosophila melanogaster*. II. Zygotic loci on the third chromosome. *Roux's Arch. Dev. Biol.* **193**, 283-295.
Kantardzhieva, A., Gosens, I., Alexeeva, S., Punte, I. M., Versteeg, I., Krieger, E., Neefjes-Mol, C. A., den Hollander, A. I., Letteboer, S. J. F., Klooster, J. et al. (2005). MPP5 recruits MPP4 to the CRB1 complex in photoreceptors. *Invest. Ophtalmol. Vis. Sci.* **46**, 2192-2201.
Kaspar, M., Schneider, M., Chia, W. and Klein, T. (2008). Klumpfuss is involved in the determination of sensory organ precursors in *Drosophila*. *Dev. Biol.* **324**, 177-191.
Keen, J. H. (1987). Clathrin assembly proteins: affinity purification and a model for coat assembly. *J. Cell Biol.* **105**, 1989-1998.
Kelly, B. T., McCoy, A. J., Späte, K., Miller, S. E., Evans, P. R., Höning, S. and Owen, D. J. (2008). A structural explanation for the binding of endocytic dileucine motifs by the AP2 complex. *Nature* **456**, 976-979.
Kempkens, Ö., Médina, E., Fernandez-Ballester, G., Özüyaman, S., Le Bivic, A., Serrano, L. and Knust, E. (2006). Computer modelling in combination with in vitro studies reveals similar binding affinities of *Drosophila* Crumbs for the PDZ domains of Stardust and *Dm*Par-6. *Eur. J. Cell Biol.* **85**, 753-767.
Kim, S., Wairkar, Y. P., Daniels, R. W. and DiAntonio, A. (2010). The novel endosomal membrane protein Ema interacts with the class C Vps-HOPS complex to promote endosomal maturation. *J. Cell Biol.* **188**, 717-734.
Klebes, A. and Knust, E. (2000). A conserved motif in Crumbs is required for E-cadherin localisation and zonula adherens formation in *Drosophila*. *Curr. Biol.* **10**, 76-85.
Klose, S., Flores-Benitez, D., Riedel, F. and Knust, E. (2013). Fosmid-based structure-function analysis reveals functionally distinct domains in the cytoplasmic domain of *Drosophila* Crumbs. *G3* **3**, 153-165.
Knust, E. and Bossinger, O. (2002). Composition and formation of intercellular junctions in epithelial cells. *Science* **298**, 1955-1959.
Kosaka, T. and Ikeda, K. (1983). Reversible blockage of membrane retrieval and endocytosis in the garland cell of the temperature-sensitive mutant of *Drosophila melanogaster*, *shibire[ts1]*. *J. Cell Biol.* **97**, 499-507.
Laprise, P., Beronja, S., Silva-Gagliardi, N. F., Pellikka, M., Jensen, A. M., McGlade, C. J. and Tepass, U. (2006). The FERM protein Yurt is a negative regulatory component of the Crumbs complex that controls epithelial polarity and apical membrane size. *Dev. Cell* **11**, 363-374.
Le Borgne, R., Bardin, A. and Schweisguth, F. (2005). The roles of receptor and ligand endocytosis in regulating Notch signaling. *Development* **132**, 1751-1762.
Letizia, A., Ricardo, S., Moussian, B., Martin, N. and Llimargas, M. (2013). A functional role of the extracellular domain of Crumbs in cell architecture and apicobasal polarity. *J. Cell Sci.* **126**, 2157-2163.
Li, Y., Wei, Z., Yan, Y., Wan, Q., Du, Q. and Zhang, M. (2014). Structure of Crumbs tail in complex with the PALS1 PDZ-SH3-GK tandem reveals a highly specific assembly mechanism for the apical Crumbs complex. *Proc. Natl. Acad. Sci. USA* **111**, 17444-17449.
Lindwasser, O. W., Smith, W. J., Chaudhuri, R., Yang, P., Hurley, J. H. and Bonifacino, J. S. (2008). A diacidic motif in human immunodeficiency virus type 1 Nef is a novel determinant of binding to AP-2. *J. Virol.* **82**, 1166-1174.
Ling, C., Zheng, Y., Yin, F., Yu, J., Huang, J., Hong, Y., Wu, S. and Pan, D. (2010). The apical transmembrane protein Crumbs functions as a tumor suppressor that regulates Hippo signaling by binding to Expanded. *Proc. Natl. Acad. Sci. USA* **107**, 10532-10537.
Lu, H. and Bilder, D. (2005). Endocytic control of epithelial polarity and proliferation in *Drosophila*. *Nat. Cell Biol.* **7**, 1232-1239.
Makarova, O., Roh, M. H., Liu, C.-J., Laurinec, S. and Margolis, B. (2003). Mammalian Crumbs3 is a small transmembrane protein linked to protein associated with Lin-7 (Pals1). *Gene* **302**, 21-29.
Maldonado-Báez, L. and Wendland, B. (2006). Endocytic adaptors: recruiters, coordinators and regulators. *Trends Cell Biol.* **16**, 505-513.
Matsui, W. and Kirchhausen, T. (1990). Stabilization of clathrin coats by the core of the clathrin-associated protein complex AP-2. *Biochemistry* **29**, 10791-10798.
Moberg, K. H., Schelble, S., Burdick, S. K. and Hariharan, I. K. (2005). Mutations in erupted, the *Drosophila* ortholog of mammalian tumor susceptibility gene 101, elicit non-cell-autonomous overgrowth. *Dev. Cell* **9**, 699-710.
Müller, U. and Wild, K. (2013). Structure and function of the APP intracellular domain in health and disease. In *Understanding Alzheimer's Disease* (ed. I. Zerr), pp. 3-22. ISBN: 978-953-51-1009-5, InTech.
Murciano-Calles, J., Corbi-Verge, C., Candel, A. M., Luque, I. and Martinez, J. C. (2014). Post-translational modifications modulate ligand recognition by the third PDZ domain of the MAGUK protein PSD-95. *PLoS ONE* **9**, e90030.
Muschalik, N. and Knust, E. (2011). Increased levels of the cytoplasmic domain of Crumbs repolarise developing *Drosophila* photoreceptors. *J. Cell Sci.* **124**, 3715-3725.
Nam, S.-C. and Choi, K.-W. (2003). Interaction of Par-6 and Crumbs complexes is essential for photoreceptor morphogenesis in *Drosophila*. *Development* **130**, 4363-4372.
Owen, D. J., Vallis, Y., Noble, M. E. M., Hunter, J. B., Dafforn, T. R., Evans, P. R. and McMahon, H. T. (1999). A structural explanation for the binding of multiple ligands by the α-adaptin appendage domain. *Cell* **97**, 805-815.
Owen, D. J., Vallis, Y., Pearse, B. M. F., McMahon, H. T. and Evans, P. R. (2000). The structure and function of the β2-adaptin appendage domain. *EMBO J.* **19**, 4216-4227.
Padash-Barmchi, M., Browne, K., Sturgeon, K., Jusiak, B. and Auld, V. J. (2010). Control of Gliotactin localization and levels by tyrosine phosphorylation and endocytosis is necessary for survival of polarized epithelia. *J. Cell Sci.* **123**, 4052-4062.

Journal of Cell Science

Pandey, K. N. (2009). Functional roles of short sequence motifs in the endocytosis of membrane receptors. *Front. Biosci.* **14**, 5339-5360.
Park, B., Alves, C. H., Lundvig, D. M., Tanimoto, N., Beck, S. C., Huber, G., Richard, F., Klooster, J., Andlauer, T. F. M., Swindell, E. C. et al. (2011). PALS1 is essential for retinal pigment epithelium structure and neural retina stratification. *J. Neurosci.* **31**, 17230-17241.
Pellikka, M., Tanentzapf, G., Pinto, M., Smith, C., McGlade, C. J., Ready, D. F. and Tepass, U. (2002). Crumbs, the *Drosophila* homologue of human CRB1/RP12, is essential for photoreceptor morphogenesis. *Nature* **416**, 143-149.
Pocha, S. M., Wassmer, T., Niehage, C., Hoflack, B. and Knust, E. (2011). Retromer controls epithelial cell polarity by trafficking the apical determinant Crumbs. *Curr. Biol.* **21**, 1111-1117.
Prybylowski, K., Chang, K., Sans, N., Kan, L., Vicini, S. and Wenthold, R. J. (2005). The synaptic localization of NR2B-containing NMDA receptors is controlled by interactions with PDZ proteins and AP-2. *Neuron* **47**, 845-857.
Reider, A. and Wendland, B. (2011). Endocytic adaptors–social networking at the plasma membrane. *J. Cell Sci.* **124**, 1613-1622.
Ribeiro, P., Holder, M., Frith, D., Snijders, A. P. and Tapon, N. (2014). Crumbs promotes expanded recognition and degradation by the SCF(Slimb/β-TrCP) ubiquitin ligase. *Proc. Natl. Acad. Sci. USA* **111**, E1980-E1989.
Richard, M., Grawe, F. and Knust, E. (2006). DPATJ plays a role in retinal morphogenesis and protects against light-dependent degeneration of photoreceptor cells in the *Drosophila* eye. *Dev. Dyn.* **235**, 895-907.
Robinson, B. S., Huang, J., Hong, Y. and Moberg, K. H. (2010). Crumbs regulates Salvador/Warts/Hippo signaling in *Drosophila* via the FERM-domain protein expanded. *Curr. Biol.* **20**, 582-590.
Rodriguez-Boulan, E. and Macara, I. G. (2014). Organization and execution of the epithelial polarity programme. *Nat. Rev. Mol. Cell Biol.* **15**, 225-242.
Roeth, J. F., Sawyer, J. K., Wilner, D. A. and Peifer, M. (2009). Rab11 helps maintain apical crumbs and adherens junctions in the *Drosophila* embryonic ectoderm. *PLoS ONE* **4**, e7634.
Roh, M. H., Fan, S., Liu, C.-J. and Margolis, B. (2003). The Crumbs3-Pals1 complex participates in the establishement of polarity in mammalian epithelial cells. *J. Cell Sci.* **116**, 2895-2906.
Röper, K. (2012). Anisotropy of Crumbs and aPKC drives myosin cable assembly during tube formation. *Dev. Cell* **23**, 939-953.
Sherrard, K. M. and Fehon, R. G. (2015). The transmembrane protein Crumbs displays complex dynamics during follicular morphogenesis and is regulated competitively by Moesin and aPKC. *Development* **142**, 2226.
Slepnev, V. I. and De Camilli, P. (2000). Accessory factors in clathrin-dependent synaptic vesicle endocytosis. *Nat. Rev. Neurosci.* **1**, 161-172.
Song, Y. and Lu, B. (2012). Interaction of Notch signaling modulator Numb with α-Adaptin regulates endocytosis of Notch pathway components and cell fate determination of neural stem cells. *J. Biol. Chem.* **287**, 17716-17728.
Soukup, S. F., Culi, J. and Gubb, D. (2009). Uptake of the necrotic serpin in *Drosophila melanogaster* via the lipophorin receptor-1. *PLoS Genet.* **5**, e1000532.
St Johnston, D. and Ahringer, J. (2010). Cell polarity in eggs and epithelia: parallels and diversity. *Cell* **141**, 757-774.
Tanentzapf, G., Smith, C., McGlade, J. and Tepass, U. (2000). Apical, lateral, and basal polarization cues contribute to the development of the follicular epithelium during *Drosophila* oogenesis. *J. Cell Biol.* **151**, 891-904.
Tepass, U. (1996). Crumbs, a component of the apical membrane, is required for zonula adherens formation in primary epithelia of *Drosophila*. *Dev. Biol.* **177**, 217-225.
Tepass, U. and Knust, E. (1990). Phenotypic and developmental analysis of mutations at the *crumbs* locus, a gene required for the development of epithelia in *Drosophila melanogaster*. *Roux's Arch. Dev. Biol.* **199**, 189-206.
Tepass, U. and Knust, E. (1993). *crumbs* and *stardust* act in a genetic pathway that controls the organization of epithelia in *Drosophila melanogaster*. *Dev. Biol.* **159**, 311-326.
Tepass, U., Theres, C. and Knust, E. (1990). *crumbs* encodes an EGF-like protein expressed on apical membranes of *Drosophila* epithelial cells and required for organization of epithelia. *Cell* **61**, 787-799.
Tepass, U., Tanentzapf, G., Ward, R. and Fehon, R. (2001). Epithelial cell polarity and cell junctions in Drosophila. *Annu. Rev. Genet.* **35**, 747-784.
Traub, L. M. (2009). Tickets to ride: selecting cargo for clathrin-regulated internalization. *Nat. Rev. Mol. Cell Biol.* **10**, 583-596.
van Rossum, A. G. S. H., Aartsen, W. M., Meuleman, J., Klooster, J., Malysheva, A., Versteeg, I., Arsanto, J.-P., Le Bivic, A. and Wijnholds, J. (2006). Pals1/Mpp5 is required for correct localization of Crb1 at the subapical region in polarized Muller glia cells. *Hum. Mol. Genet.* **15**, 2659-2672.
Weavers, H., Prieto-Sánchez, S., Grawe, F., Garcia-López, A., Artero, R., Wilsch-Bräuninger, M., Ruiz-Gómez, M., Skaer, H. and Denholm, B. (2009). The insect nephrocyte is a podocyte-like cell with a filtration slit diaphragm. *Nature* **457**, 322-326.
Wei, Z., Li, Y., Ye, F. and Zhang, M. (2015). Structural basis for the phosphorylation-regulated interaction between the cytoplasmic tail of cell polarity protein Crumbs and the actin-binding protein Moesin. *J. Biol. Chem.* **290**, 11384-11392.
Whiteman, E. L., Fan, S., Harder, J. L., Walton, K. D., Liu, C.-J., Soofi, A., Fogg, V. C., Hershenson, M. B., Dressler, G. R., Deutsch, G. H. et al. (2014). Crumbs3 is essential for proper epithelial development and viability. *Mol. Cell. Biol.* **34**, 43-56.
Wigglesworth, V. B. (1942). *The Principles of Insect Physiology*. London: Methuen & Co. Ltd.
Windler, S. L. and Bilder, D. (2010). Endocytic internalization routes required for delta/notch signaling. *Curr. Biol.* **20**, 538-543.
Wodarz, A., Hinz, U., Engelbert, M. and Knust, E. (1995). Expression of Crumbs confers apical character on plasma membrane domains of ectodermal epithelia of *Drosophila*. *Cell* **82**, 67-76.
Xiao, Z., Patrakka, J., Nukui, M., Chi, L., Niu, D., Betsholtz, C., Pikkarainen, T., Vainio, S. and Tryggvason, K. (2011). Deficiency in Crumbs homolog 2 (Crb2) affects gastrulation and results in embryonic lethality in mice. *Dev. Dyn.* **240**, 2646-2656.
Xu, T. and Rubin, G. M. (1993). Analysis of genetic mosaics in developing and adult *Drosophila* tissues. *Development* **117**, 1223-1237.
Zhang, J., Petit, C. M., King, D. S. and Lee, A. L. (2011). Phosphorylation of a PDZ domain extension modulates binding affinity and interdomain interactions in postsynaptic density-95 (PSD-95) protein, a membrane-associated guanylate kinase (MAGUK). *J. Biol. Chem.* **286**, 41776-41785.
Zhou, B., Wu, Y. and Lin, X. (2011). Retromer regulates apical-basal polarity through recycling Crumbs. *Dev. Biol.* **360**, 87-95.
Zou, J., Wang, X. and Wei, X. (2012). Crb apical polarity proteins maintain zebrafish retinal cone mosaics via intercellular binding of their extracellular domains. *Dev. Cell* **22**, 1261-1274.